31st Annual International Conference of the IEEE EMBS
Minneapolis, Minnesota, USA, September 2-6, 2009

# Characterization of Pancreatic Cancer and Intra-abdominal Lymph Node Malignancy using Spectrum Analysis of Endoscopic Ultrasound Imaging

Ronald E. Kumon, Ph.D., *Member, IEEE*, Michael J. Pollack, M.D., Ashley L. Faulx, M.D., Kayode Olowe, M.D., Farees T. Farooq, M.D., Victor K. Chen, M.P.H., M.D., Yun Zhou, Ph.D., *Member, IEEE,* Richard C. K. Wong, M.D., Gerard A. Isenberg, M.D., Michael V. Sivak, M.D., Amitabh Chak, M.D., and Cheri X. Deng, Ph.D., *Member, IEEE*

*Abstract*—**This study assessed the ability of spectral analysis of endoscopic ultrasound (EUS) RF signals acquired in humans *in vivo* to distinguish between (1) benign and malignant intra-abdominal and mediastinal lymph nodes and (2) pancreatic cancer, chronic pancreatitis, and normal pancreas. Mean midband fit, slope, intercept, and correlation coefficient from a linear regression of the calibrated RF power spectra were computed over regions of interest defined by the endoscopist. Linear discriminant analysis was then performed to develop a classification of the resulting spectral parameters. For lymph nodes, classification based on the midband fit and intercept provided 67% sensitivity, 82% specificity, and 73% accuracy for malignant vs. benign nodes. For pancreas, classification based on midband fit and correlation coefficient provided 95% sensitivity, 93% specificity, and 93% accuracy for diseased vs. normal pancreas and 85% sensitivity, 71% specificity, and 85% accuracy for pancreatic cancer vs. chronic pancreatitis. These promising results suggest that mean spectral parameters can provide a non-invasive method to quantitatively characterize pancreatic cancer and lymph malignancy *in vivo*.**

## I. Introduction

Cancers of the digestive system accounted for 19% of the 1.44 estimated million cancer cases and 24% of the 566,000 estimated cancer deaths in the U.S. during 2008 [1]. A disproportionate level of mortality arises from several cancers of gastrointestinal (GI) organs that are difficult to detect or treat, particularly pancreatic cancer, but survival rates are better when the disease can be found and properly characterized when it is still localized to the organ or nearby tissue. Hence emerging technology that can improve the ability to detect pathologies, distinguish benign from malignant tumors, identify the spread of cancer to lymph nodes, and properly identify the overall stage of the cancer will provide valuable information which can help to improve the effectiveness of cancer therapies.

Endoscopic ultrasound (EUS) provides clinicians the ability to image tissue structures beyond the luminal surface of the GI tract [2]. It can be used to determine the depth of invasion of GI tumors as well as to identify regional lymph nodes. In addition, organs in close proximity to the GI tract lumen, such as the pancreas and liver, can be imaged with a high resolution, often exceeding that of radiographic imaging modalities. For pancreatic cancer, a major advantage of EUS is negative predictive value approaching 100%, indicating that the absence of a focal mass reliably excludes pancreatic cancer [3]. EUS can also be controlled in real-time, which enables it to be used for guidance of needle biopsies of surrounding lymph nodes.

Effective use of EUS imaging depends on judgments regarding changes in the sonographic characteristics of the imaged areas of interest. These characteristics typically include size, morphology, relative echogenicity, and level of homo- or heterogeneity. Deciphering these characteristics in real-time is operator-dependent and contingent on the ability of the naked eye to detect grayscale nuances. Clinically, this task is difficult in both the contexts of identifying pancreatic cancers in the setting of chronic pancreatitis [4] and differentiating benign from malignant lymph nodes [5, 6]. An accurate, objective means of differentiating benign or inflammatory from malignant tissue would improve the diagnostic accuracy of EUS, reduce the need for multiple needle passes while targeting lesions for biopsy, and thereby significantly impact patient care.

EUS systems operate in pulse-echo mode, whereby a transducer transmits a pulse and then receives the resulting series of radio-frequency (RF) signals that return. As the pulse propagates through tissue, it is reflected and scattered by interfaces and inhomogeneities in the tissue and attenuated by thermoviscous absorption. Conventional B-mode ("brightness") images represent the echo RF signals by displaying them in an image format with grayscale values that are proportional to the magnitude of the video envelope of the signal. This nonlinear procedure removes signal phase information that may include features related to tissue microstructure [7]. By transforming the data from the time domain to the frequency (spectral) domain and then using

Manuscript received April 7, 2009. This work was supported in part by the Ohio Wright Center of Innovation/Biomedical Research and Technology Transfer Grant "Biomedical structural, functional and molecular imaging enterprise." A.C. was supported in part by a K24 Midcareer Award in Patient Oriented Research, National Institutes of Health (Grant DK002800). F.T.F. and R. E.K. were supported in part by an ASGE Research, Outcomes, and Effectiveness Award.

R.E.K.,* Y.Z., and C.X.D. are with the Department of Biomedical Engineering, University of Michigan, Ann Arbor, Michigan, USA (*phone: 734–763–5448; e-mail: kumon@ieee.org).

M.J.P., A.L.F., K.O., F.T.F., V.K.C., R.C.K.W., G.A.I., M.V.S., and A.C.* are or were with Division of Gastroenterology, University Hospitals Case Medical Center and Case Western Reserve University, Cleveland, Ohio, USA (*phone: 216–844–5385; e-mail: amitabh.chak@case.edu).

calibration procedures to remove artifacts from the transducer and electronics, quantitative measurements of ultrasound backscatter may be derived for any given region of interest to reveal critical signal features. The resulting quasi-linear calibrated spectra can be characterized by their slope, intercept, correlation coefficient, and midband fit (value of the regression line at the center frequency), which can then be correlated to tissue characteristics. Such backscatter measurements have been shown to relate to the size, concentration, and acoustic impedance of the scatterers [8], thereby allowing different tissue types to be distinguished (e.g., a malignant tumor scatters differently than normal tissue because of its different microstructure [9]). In the context of GI cancer, ex vivo studies of lymph node metastases of colorectal cancer have shown that spectral ultrasound backscatter analysis performed better than B-mode ultrasound [10] even when multiple B-mode sonographic parameters were considered [11].

The study reported herein employs spectral analysis of backscattered signals from EUS imaging *in vivo* to quantitatively characterize the differences between (1) normal pancreas (NP), chronic pancreatitis (CP), and pancreatic cancer (PC) and (2) benign and malignant intra-abdominal lymph nodes. A portion of the raw data reported in this paper was analyzed for a previous pilot study [12], but it is re-analyzed here in light of an improved calibration procedure and new data from 24 additional patients. A linear discriminant analysis (LDA) was then performed to classify the data, and receiver-operating characteristic (ROC) curves were calculated to evaluate the classification.

## II. Materials and Methods

### A. Patients and clinical protocols

A total of 43 subjects (16 men and 27 women; mean age 66, range 36–90) already scheduled for esophagogastroduodenoscopy (EGD) with EUS were enrolled in the study. In this procedure, the fiber-optic endoscope is inserted through the patient's mouth and moved down the esophagus to the stomach and duodenum. The subjects were given a sedative and analgesic, and a local anesthetic was applied to suppress the gag reflex during insertion. Due to system limitations, different endoscopes were used for RF data acquisition and biopsies. As the data acquisition process does not affect the procedure itself, a waiver of patient consent for this study was granted by our institutional review board. Pancreas cases were diagnosed as NP, CP, or PC while lymph nodes were diagnosed as benign or malignant, both using detailed criteria reported previously [12] based on the literature [5, 13, 14]. In brief, malignant cases were determined primarily based on positive biopsy, while non-malignant cases were determined mainly from EUS appearance in patients not referred for cancer and with no cancer after 1 year. In some cases, images were also taken in areas outside of the organ of primary interest to act as normal controls.

### B. Data acquisition and analysis

For this study, the Olympus Exera EU-M60 ultrasound center was used with the Olympus GF-UM160 ultrasonic gastrovideoscope to obtain the data. With permission from Olympus America, the ultrasound center was modified with a special output port to allow the RF data to be acquired without affecting the system's normal operation. The endoscope tip contains a lens for obtaining optical images and a transducer that spins about the axis of the scope in the lumen, thereby creating B-scan cross-sectional images, each consisting of 256 consecutive lines of RF data. The broadband, single-element, focused transducer was set to operate in C5 mode (6 MHz center freq., 3.415 kHz PRF, 20 mm focal distance). The RF data for a full revolution were captured using a LeCroy LT372 oscilloscope in 8-bit mode at sampling rates of 100 or 200 MHz and were obtained prior to time-gain compensation and other processing used to create the B-mode image. In each case, the B-scan image generated by the Olympus system was saved for purposes of comparison with the image reconstructed off-line from the RF data later. These two images could not be acquired simultaneously due to technical issues, but were taken as close together as possible in time.

The RF data were imported into our custom-designed, MATLAB-based analysis software with a graphical user interface for image reconstruction and data processing. The B-scan image from the RF data was reconstructed and then oriented to match the system image using identifiable landmarks on the image. Prior to RF data analysis, regions of interest (ROIs) were identified and manually segmented by the endoscopist on the system image. The ROIs were then independently translated onto the reconstructed image to select corresponding segments of RF data. Each sector-shaped area was sized to be as large as possible within the designated ROIs. The power spectrum was calculated for the signals of each RF A-scan within the ROI, by taking the FFT of the data gated by a series of sliding Hamming windows of 1.5 μs (~2.3 mm in space), each offset by 0.1 μs.

### C. Spectrum calibration

To remove artifacts associated with the composite transfer function of the electronic pulser/receiver and transducer, calibration was performed by dividing the tissue power spectrum by the calibration spectrum from a high-reflectivity interface. The calibration spectrum was obtained in the current study using an acrylic plastic cylinder (5.08 cm inner diam.) filled with a custom-made gelatin-phantom in the form of a cylindrical annulus (0.635 cm inner diam.) with attenuation of 0.7 dB/MHz/cm. The phantom prevented signal saturation from the receiver electronics of the EUS system. The central hole in the gelatin phantom was filled with water prior to the insertion of the endoscope transducer, and the endoscope's balloon was inflated with water until it was in full contact with the phantom. The orientation of the endoscope tip was then manually adjusted to ensure that the endoscope was centered and parallel to the symmetry axis of the cylinder. The spectrum was broad, fairly uniform (15 dB bandwidth over 2–10 MHz), and generally consistent with the frequency characteristics specified by the manufacturer. The resulting spectrum was used for calibration of the new RF data and the re-analysis of the pilot study data.

### D. Statistical analysis

The spectral parameters generated from each window were averaged over each ROI. The resulting values were then analyzed using Student's *T*-test for the two tissue types in the lymph-node data and a one-way ANOVA for the three tissue types in the pancreas data using the Bonferroni criterion for multiple comparisons. Once parameters were identified that provided statistically significant differences between group means, LDA was performed to classify the data using equal prior probabilities for each group and the within-groups covariance matrix. The leave-one-out approach was used for cross-validation. All statistical calculations were performed using SPSS 16. A binormal ROC curve was then fit to the resulting discriminant scores using the maximum likelihood estimation routine of ROCKIT 1.1B2 [15]. Classification was assessed by computing the area under the curve (AUC) from ROCKIT.

## III. Results

### A. Lymph nodes

RF data from 16 subjects (7 men and 9 women, mean age 66, range 48–90) were examined, yielding a total of 26 ROIs in the resulting images. Only the midband fit and intercept showed statistically significant differences between the two groups at the $p = 0.05$ level (Table I), and so only these parameters were used for the linear discriminant analysis. Table II shows the results of the classification. The leave-one-out, cross-validated classification had sensitivity of 67%, specificity of 82%, positive predictive value (PPV) of 83%, negative predictive value (NPV) of 75%, and overall accuracy of 73%. Figure 1 shows the corresponding binormal ROC curve with AUC = 0.90. The use of midband fit and intercept together provided slightly higher AUC than either parameter alone, although the differences were not statistically significant. In all cases, the classification was significantly better than guessing (AUC = 0.5) with $p < 0.01$.

### B. Pancreas

RF data from 41 subjects (14 men and 27 women, mean age 66, range 36–85) were acquired for total of 60 ROIs in the resulting images. Only midband fit and correlation coefficient $R^2$ showed statistically significant differences between all three groups at the $p = 0.05$ level (Table III), and so only these parameters were used for the LDA. The resulting classification matrix from the three-group LDA is shown in Table IV. Additional two-group LDAs were performed to compare classification for (i) normal (NP) vs non-normal (PC+CP) and (ii) PC vs. CP excluding NP. Figure 2 shows the corresponding binormal ROC curves for each comparison. When NP is compared to diseased pancreas, the classification had sensitivity of 95%, specificity of 93%, PPV of 86%, NPV of 97%, overall accuracy of 93%, and ROC AUC = 0.99 (solid line in Fig. 2). When PC is compared to CP excluding NP, the classification had sensitivity of 85%, specificity of 71%, PPV of 85%, NPV of 86%, overall accuracy of 85%, and

TABLE I
LYMPH NODES DATA: DESCRIPTIVE STATISTICS & HYPOTHESIS TESTING

| Type | Midband Fit (dB) | Intercept (dB) |
|---|---|---|
| Benign ($n = 15$) | −43.8±6.6 | −36.5±6.8 |
| Malignant ($n = 11$) | −51.8±3.2 | −46.3±7.1 |
| $p$-value | < 0.001 | < 0.002 |

TABLE II
LYMPH NODES DATA: LINEAR DISCRIMINANT ANALYSIS RESULTS

| Actual State | Predicted State | |
|---|---|---|
| | Benign | Malignant |
| Benign | 10 | 5 |
| Malignant | 2 | 9 |

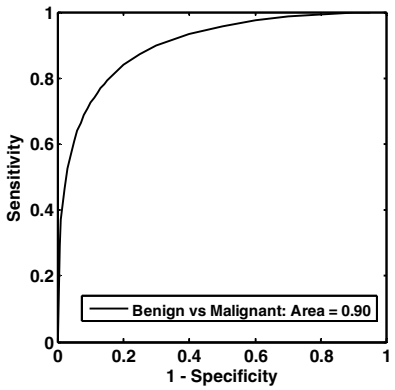


Fig. 1. Binormal ROC curve for LDA of lymph nodes data.

TABLE III
PANCREAS DATA: DESCRIPTIVE STATISTICS & HYPOTHESIS TESTING

| Type | Midband Fit (dB) | Corr. Coeff. $R^2$ |
|---|---|---|
| NP ($n = 40$) | −41.5±3.4 | 0.40±0.12 |
| PC ($n = 13$) | −53.2±1.1 | 0.16±0.04 |
| CP ($n = 7$) | −50.2±2.1 | 0.26±0.07 |
| NP vs. PC $p$-value | < 0.001 | < 0.001 |
| NP vs. CP $p$-value | < 0.001 | < 0.01 |
| PC vs. CP $p$-value | < 0.05 | < 0.05 |

TABLE IV
PANCREAS DATA: LINEAR DISCRIMINANT ANALYSIS RESULTS

| Actual State | Predicted State | | |
|---|---|---|---|
| | NP | PC | CP |
| NP | 36 | 0 | 4 |
| PC | 0 | 12 | 1 |
| CP | 0 | 2 | 5 |

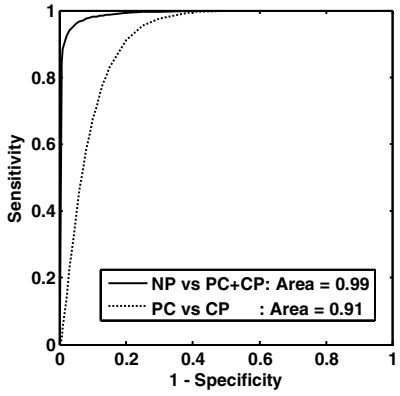


Fig. 2. Binormal ROC curve for LDA of pancreas data.

ROC AUC = 0.91 (dotted line in Fig. 2). The LDA indicated that most of the discrimination resulted from the midband fit; as such, the use of midband fit and $R^2$ provided comparable AUC to midband fit alone. In all cases, the classification was significantly better than guessing (AUC = 0.5) with $p < 0.01$.

## IV. Discussion

B-mode imaging uses only the amplitude of the envelope of the B-mode RF data to produce the grayscale encoding in the image, ignoring the frequency and phase information of the signal that may include potentially useful information about tissue properties. The primary advantage of the spectral analysis of RF signals over conventional B-mode imaging is that the spectral analysis permits objective and quantitative measurements of tissue properties by reducing the instrument-, setting-, and user-dependences inherent in grayscale B-mode interpretation. As the spectral analysis procedure uses information already available in existing EUS systems, clinical implementation can be done with minimal modification to current equipment and procedures. The procedure is also applicable to systems with digital signals and linear arrays.

Previous analyses of ultrasound backscatter spectra have shown their utility to extract potentially useful information about tissue microstructure as characterized through effective acoustic scatterers in the tissue [7]. The slope of the spectrum depends primarily on scatterer size, while the midband fit and intercept contain information about the scatterer concentration and relative acoustic impedance between the scatterers and surrounding tissue. Our results show that slope is not as effective as midband fit and intercept for differentiating between malignant and non-malignant tissue; this suggests that scatterer size is a less important factor than scatterer concentration and acoustic impedance for tissue differentiation in the current applications. For the pancreas data, the reduced midband fit between NP and PC is consistent with the typically reduced echogenicity of tumors relative to surrounding tissue. However, these measurements provide a quantitative assessment of the difference.

Additional work is necessary to fully demonstrate the effectiveness of the technique. Results may be improved by acquiring RF data with the same echoendoscope used to guide the needle biopsy; such a study is already in progress with a new system. Ideally, future systems will allow clinicians to acquire real-time images that are “digitally stained” with coloration indicating the probability of disease states based on spectral classification, and thereby provide improved diagnosis of pancreatic lesions and lymph nodes during EUS imaging and EUS-guided needle biopsies.

## V. Conclusion

The results of this study indicate that mean spectral parameters derived from ultrasound backscatter measurements in vivo can provide a method to discriminate between (1) benign and malignant lymph nodes and (2) between normal pancreas, chronic pancreatitis, and pancreatic cancer. Additional work is needed to expand these encouraging results.


## Acknowledgment

We would like to thank Olympus Corporation for making the RF data available, Brian Wolf for his technical assistance, and Jingping Xu for the calibration phantom.


## References


[1] American Cancer Society, "Cancer Facts & Figures," American Cancer Society, Atlanta 2008.

[2] A. McLean and P. Fairclough, "Endoscopic ultrasound--current applications," Clin Radiol, vol. 51, pp. 83-98, 1996.

[3] A. Saftoiu and P. Vilmann, "Role of endoscopic ultrasound in the diagnosis and staging of pancreatic cancer," J Clin Ultrasound, vol. 37, pp. 1-17, 2009.

[4] M. S. Bhutani, F. G. Gress, M. Giovannini, R. A. Erickson, M. F. Catalano, A. Chak, P. H. Deprez, D. O. Faigel, and C. C. Nguyen, "The No Endosonographic Detection of Tumor (NEST) Study: a case series of pancreatic cancers missed on endoscopic ultrasonography," Endoscopy, vol. 36, pp. 385-9, 2004.

[5] M. F. Catalano, E. Alcocer, A. Chak, C. C. Nguyen, I. Raijman, J. E. Geenen, S. Lahoti, and M. V. Sivak, Jr., "Evaluation of metastatic celiac axis lymph nodes in patients with esophageal carcinoma: accuracy of EUS," Gastrointest Endosc, vol. 50, pp. 352-6, 1999.

[6] A. Kanamori, Y. Hirooka, A. Itoh, S. Hashimoto, H. Kawashima, K. Hara, H. Uchida, J. Goto, N. Ohmiya, Y. Niwa, and H. Goto, "Usefulness of contrast-enhanced endoscopic ultrasonography in the differentiation between malignant and benign lymphadenopathy," Am J Gastroenterol, vol. 101, pp. 45-51, 2006.

[7] F. L. Lizzi, E. J. Feleppa, S. K. Alam, and C. X. Deng, "Ultrasonic spectrum analysis for tissue evaluation," Pattern Recog Lett, vol. 24, pp. 637-658, 2003.

[8] F. L. Lizzi, M. Ostromogilsky, E. J. Feleppa, M. C. Rorke, and M. M. Yaremko, "Relationship of ultrasonic spectral parameters to features of tissue microstructure," IEEE Trans Ultrason Ferroelectr Freq Control, vol. 34, pp. 319-29, 1987.

[9] M. L. Oelze, W. D. O'Brien, Jr., J. P. Blue, and J. F. Zachary, "Differentiation and characterization of rat mammary fibroadenomas and 4T1 mouse carcinomas using quantitative ultrasound imaging," IEEE Trans Med Imaging, vol. 23, pp. 764-71, 2004.

[10] T. Noritomi, J. Machi, E. J. Feleppa, E. Yanagihara, and K. Shirouzu, "In vitro investigation of lymph node metastasis of colorectal cancer using ultrasonic spectral parameters," Ultrasound Med Biol, vol. 24, pp. 235-43, 1998.

[11] T. Tateishi, J. Machi, E. J. Feleppa, A. J. Oishi, N. L. Furumoto, R. H. Oishi, L. J. McCarthy, E. Yanagihara, and K. Shirouzu, "In vitro investigation of detectability of colorectal lymph nodes and diagnosis of lymph node metastasis in colorectal cancer using B-mode sonography," J Clin Ultrasound, vol. 32, pp. 1-7, 2004.

[12] R. E. Kumon, K. Olowe, A. L. Faulx, F. T. Farooq, V. K. Chen, Y. Zhou, R. C. Wong, G. A. Isenberg, M. V. Sivak, A. Chak, and C. X. Deng, "EUS spectrum analysis for in vivo characterization of pancreatic and lymph node tissue: a pilot study," Gastrointest Endosc, vol. 66, pp. 1096-106, 2007.

[13] N. Schmulewitz, S. M. Wildi, S. Varadarajulu, S. Roberts, R. H. Hawes, B. J. Hoffman, V. Durkalski, G. A. Silvestri, M. I. Block, C. Reed, and M. B. Wallace, "Accuracy of EUS criteria and primary tumor site for identification of mediastinal lymph node metastasis from non-small-cell lung cancer," Gastrointest Endosc, vol. 59, pp. 205-12, 2004.

[14] M. B. Wallace and R. H. Hawes, "Endoscopic ultrasound in the evaluation and treatment of chronic pancreatitis," Pancreas, vol. 23, pp. 26-35, 2001.

[15] University of Chicago, "Receiver Operating Characteristic program software downloads. http://xray.bsd.uchicago.edu/krl/KRL_ROC/software_index.htm."